Diversity of fate outcomes in cell pairs under lateral inhibition

Nara Guisoni[1,2,*], Rosa Martinez-Corral[1,*], Jordi Garcia Ojalvo[1,#], and Joaquín de Navascués[3,#]

[1] Department of Experimental and Health Sciences, Universitat Pompeu Fabra, Barcelona Biomedical Research Park (PRBB), Dr. Aiguader 88, 08003 Barcelona, Spain.

[2] Instituto de Física de Líquidos y Sistemas Biológicos, CONICET & Universidad Nacional de La Plata, Calle 59-789, 1900 La Plata, Argentina.

[3] European Cancer Stem Cell Research Institute, School of Biosciences, Cardiff University, Hadyn Ellis Building, Maindy Road, Cardiff CF24 4HQ, UK.

[*] Equal contribution

[#] Correspondence: denavascuesj@cardiff.ac.uk, jordi.g.ojalvo@upf.edu

Key words: Lateral inhibition, Notch-Delta signalling, symmetric cell division, intestinal stem cells, neutral competition

Running title: Symmetry in lateral inhibition

Summary statement: Notch/Delta-mediated lateral inhibition in cell pairs can result in symmetric signalling depending on the activation threshold, which can modulate cell-fate decisions depending on contact area.

Abstract

Cell fate determination by lateral inhibition via Notch/Delta signalling has been extensively studied. Most formalised models consider Notch/Delta interactions in fields of cells, with parameters that typically lead to symmetry breaking of signalling states between neighbouring cells, commonly resulting in salt-and-pepper fate patterns. Here we consider the case of signalling between isolated cell pairs, and find that the bifurcation properties of a standard mathematical model of lateral inhibition can lead to stable symmetric signalling states. We apply this model to the adult intestinal stem cell (ISC) of *Drosophila*, whose fate is stochastic but dependent on the Notch/Delta pathway. We observe a correlation between signalling state in cell pairs and their contact area. We interpret this behaviour in terms of the properties of our model in the presence of population variability in signalling thresholds. Our results suggest that the dynamics of Notch/Delta signalling can contribute to explain stochasticity in stem cell fate decisions, and that the standard model for lateral inhibition can account for a wider range of developmental outcomes than previously considered.

Introduction

The Notch/Delta signalling pathway is one of the main regulators of cellular differentiation during development and adult tissue maintenance (reviewed in (Artavanis-Tsakonas et al., 1999; Ehebauer et al., 2006; Koch et al., 2013). It often drives mutually inhibitory interactions between cells, acting as a gate for differentiation. This mode of action has been termed lateral inhibition, and has been the object of experimental study as well as mathematical formalisation for decades (see, for instance, Othmer and Scriven, 1971; Collier et al., 1996; Sprinzak et al., 2011; Petrovic et al., 2014). Quantitative models of lateral inhibition usually involve a field of cells expressing initially similar amounts of the receptor Notch and its membrane-bound ligand Delta. Delta trans-activates Notch in neighbouring cells and Notch, once activated, reduces in turn the ability of the cell to signal through Delta, leading to a state of mutual repression. This symmetry (and cell fate equivalence) is eventually broken by enforced biases and/or stochastic variation in Notch/Delta levels (Collier et al., 1996; Plahte, 2001; reviewed in Simpson, 2001) resulting in extended fine-grained spacing patterns (Othmer and Scriven, 1971; Collier et al., 1996; see also Shaya and Sprinzak, 2011) that have been experimentally characterized in depth in real developmental systems (reviewed in Greenwald, 1998; Arias and Stewart, 2002). In contrast, little attention has been paid so far to the effect of lateral inhibition in isolated cell pairs, beyond the trivial expectation that symmetry breaking will eventually take place, leading to cells taking opposing fates (see for instance, Collier et al., 1996; Rouault and Hakim, 2012). However there has been no formal investigation of whether alternative steady states are possible, perhaps due to the lack of an experimental model to relate it to.

The cellular homeostasis of the adult *Drosophila* midgut can provide this experimental scenario, as in this tissue Notch/Delta signalling occurs mostly in isolated pairs of cells (Ohlstein and Spradling, 2006; de Navascués et al., 2012; Goulas et al., 2012) (Fig.1A). The fly's intestinal lining is maintained by intestinal stem cells (ISCs), which divide to both self-renew and provide

committed progenitors. Progenitors specialise in producing either nutrient-absorbing enterocytes or secretory enteroendocrine cells (Micchelli and Perrimon, 2006; Ohlstein and Spradling, 2006; Zeng and Hou, 2015; Guo and Ohlstein, 2015). The precursors of enterocytes, called enteroblasts (EBs) are frequently found forming pairs with ISCs (Fig. 1A,B). These pairs are thought to result from an earlier division of an ISC and subsequent fate allocation by Notch signalling, before a new division or terminal differentiation event takes place (Goulas et al., 2012; de Navascués et al., 2012). Importantly, ISC divisions in the enterocyte lineage result in either asymmetric fate (one ISC and an EB), or symmetric self-renewal (two ISCs) or differentiation (two EBs), which globally result in balanced, homeostatic proportions (de Navascués et al., 2012) (Fig. 1C-E). This mode of tissue maintenance, whereby the balance between stem cell self-renewal and differentiation is achieved at the population level rather than within every stem cell lineage, is termed neutral competition (Klein and Simons, 2011) and is found in a growing number of self-renewing adult tissues (Simons and Clevers, 2011). While no molecular mechanism has been fully elucidated so far for any case of neutral competition, in the fly gut it has been proposed to arise from lateral inhibition mediated by Notch/Delta (de Navascués et al., 2012), a pathway known to define the fate of the ISC offspring (Ohlstein and Spradling, 2006; Micchelli and Perrimon, 2006; Bardin et al., 2010).

Here we explore the capacity of a standard model of lateral inhibition acting in pairs of interacting cells to result in steady states with different signalling states (either symmetric or asymmetric) coexisting in the tissue. We find that this is indeed possible, provided there is population-wide variation of signalling thresholds. Next, we turn to the *Drosophila* midgut and find that the tissue displays high variability of contact area between pairs of ISC/EB cells, which can be associated to an effective heterogeneity in signalling thresholds between pairs of cells. When contrasting this variability with the distribution of fate combinations in pairs of ISC/EB cells, we find a correlation between contact area of specific cell pairs and their fate profile. Moreover our model is

able to reproduce the distribution of fate outcomes given the contact area distribution.

Our results expand the repertoire of possible outputs of a system governed by lateral inhibition, and connect this mode of signalling with a mode of stem-cell based tissue maintenance (neutral competition) that is highly relevant in adult tissue homeostasis and tumourigenesis (Simons and Clevers, 2011; Vermeulen et al., 2013; Baker et al., 2014), and whose molecular regulation is poorly understood.

Materials and Methods

The model: lateral inhibition mediated by Notch-Delta interaction

We consider that the rate of Notch activation in a cell is an increasing function of Delta concentration on its neighbour (signalling), and that the rate of Delta expression is a decreasing function of the level of activated Notch in the same cell (inhibition). We represent these interactions by means of a standard mathematical model of Notch/Delta signalling (Collier et al., 1996) between pairs of cells, which is given by:

$$\frac{d\overline{N}_1}{dt} = \alpha f(\overline{D}_2) - \delta_N \overline{N}_1, \quad (1)$$

$$\frac{d\overline{D}_1}{dt} = \beta g(\overline{N}_1) - \delta_D \overline{D}_1, \quad (2)$$

$$\frac{d\overline{N}_2}{dt} = \alpha f(\overline{D}_1) - \delta_N \overline{N}_2, \quad (3)$$

$$\frac{d\overline{D}_2}{dt} = \beta g(\overline{N}_2) - \delta_D \overline{D}_2. \quad (4)$$

Here $\overline{N}_{1,2}$ represent the levels of Notch activity in cells 1 and 2, and $\overline{D}_{1,2}$ are the concentrations of Delta in each cell. α and β are the maximal production rates of Notch and Delta, respectively, whereas δ_N and δ_D are their corresponding degradation rates. The production terms for Notch (*f*) and Delta (*g*) are given by the Hill functions

$$f(\overline{D}) = \frac{\overline{D}^r}{K_N^r + \overline{D}^r} \text{ and } g(\overline{N}) = \frac{1}{1+(\overline{N}/K_D)^h}, \quad (5)$$

where the first function represents the signalling effect of Delta on the neighbouring cell, and the second corresponds to the inhibition of Delta expression by activated Notch in the same cell. K_N is the threshold of Notch activation by neighbouring Delta, K_D is the threshold of Delta inhibition by Notch in the same cell, and the coefficients r and h represent the cooperative character of the two aforementioned processes. Similarly to Collier et al, (1996) we rewrite Eqns 1- 4 in dimensionless form as:

$$\frac{dN_{1,2}}{dt} = \frac{D_{2,1}^r}{a^r + D_{2,1}^r} - N_{1,2}, \qquad \frac{dD_{1,2}}{dt} = \nu\left(\frac{1}{1+\left(\frac{N_{1,2}}{b}\right)^h} - D_{1,2}\right) \tag{6}$$

The parameter ν is the ratio between the degradation rates of Delta and Notch, δ_D/δ_N. a and b are the dimensionless thresholds for Notch activation by Delta in the neighboring cell, and Delta inhibition by Notch in the same cell, respectively,

$$a \equiv \frac{K_N \delta_D}{\beta} \text{ and } b \equiv \frac{K_D \delta_N}{\alpha}. \tag{7}$$

a and b are referred to as the activation and inhibition thresholds, and their values set the location of the half-maximal points of the Hill functions in Eqn 6.

Steady states and cell fate identification

The system of equations from Eqn 6 has a homogeneous steady state in which Notch and Delta have the same values in the two cells:

$$N^* = f(D^*), \qquad \mathrm{D}^* = g(N^*)$$

This state corresponds to a situation in which both cells in the pair have the same fate. The stability boundary of this homogeneous steady state can be calculated using standard methods (Collier et al., 1996), and is represented by a dotted grey line in Fig. 2A. Above this line the homogeneous state is stable. Below it, a heterogeneous stable steady state appears in which the values of Notch and Delta are different between the two cells:

$$N_1^* = f(D_2^*), \qquad D_1^* = g(N_1^*),$$

$$N_2^* = f(D_1^*), \qquad D_2^* = g(N_2^*),$$

In parallel with this classification of steady states, a cell is considered to be Notch positive when the level of Notch surpasses a certain threshold N_{thr} (considered here to be 0.1), and Notch negative in the opposite case. In the case of the *Drosophila* midgut, a Notch positive cell would correspond to an EB, and a Notch negative cell to an ISC. In that way, a homogeneous steady state can represent either an ISC/ISC pair (symmetric Notch negative) or an EB/EB pair (symmetric Notch positive). Most heterogeneous steady states, in turn, correspond to an ISC/EB pair, although heterogeneous states in which both values of Notch lie below (or above) the threshold N_{thr} still represent symmetric ISC/ISC (or EB/EB) pairs. This is reflected in Fig. 2A through the difference between the stability boundary (dotted grey line) and the boundaries between the fate-pair domains shown in colour code.

Dynamical behaviour

We investigate the temporal evolution of the model by solving numerically the Equations (6). For this purpose we use a finite difference approximation (two-stage Runge-Kutta; LeVeque, 2007). In our calculations, we are considering $r=h=2$ and $\delta_N=\delta_D$, as in previous works (Collier et al., 1996 ; Sprinzak et al., 2010). Cells are considered initially as negative for Notch activation, with similar initial levels of Notch and Delta ($N_1(t=0)=0.05$, $N_2(t=0)=0.06$, $D_1(t=0)=0.90$, $D_2(t=0)=0.91$ in dimensionless units).

Drosophila culture and strains

Adult flies were raised in standard cornmeal medium, collected daily and maintained in fresh vials with added yeast (food replaced every 24-48h) until dissection at 4-6 days of age.

EBs were identified by co-expression of an enhancer trap reporter of the undifferentiation marker *escargot* (FlyBase: *P{PTT-GB}esg*^{YB0232}; Quiñones-Coello et al., 2007) and the synthetic Notch transcriptional activity reporter *GBE-Su(H)-LacZ* (FlyBase: *P{Ddc.E(spl)m8-HLH-lacZ.Gbe}*; Bray and

159 Furriols, 2001), while ISCs were identified by expression of the *esg* reporter
160 alone (Micchelli and Perrimon, 2006; Ohlstein and Spradling, 2006) (Fig. 1A).

161 *Immunohistofluorescence and imaging*

162 Immunofluorescence was performed essentially as described in (Bardin et al.,
163 2010) but with a heat-fixation step (Miller et al., 1989).

164 Primary antibodies were: chicken anti-*β*-Galactosidase (Abcam ab9361,
165 1:200), rabbit anti-GFP (Abcam ab6556, 1:200), anti-Arm (mAb N2-7A1,
166 Developmental Studies Hybridoma Bank, 1:50), sheep anti-Notch (Muñoz-
167 Descalzo et al., 2011; 1:1000). Secondary antibodies conjugated with Alexa
168 fluorophores were from Invitrogen (1:500).

169 Confocal stacks were obtained in a Zeiss LSM 710 with an EC Plan-Neofluar
170 40X oil immersion objective (numerical aperture 1.3), with voxel size
171 0.21x0.21x1.00 or 0.14x0.14x0.42 *μ*m (XYZ) for the quantification of contact
172 area (with no oversampling in Z) and Notch distribution, respectively.

173 *Image analysis*

174 To measure contact area, stacks were analysed with a combination of ImageJ
175 macros and python scripts to (1) manually identify all esg-GFP$^+$ cells in a z-
176 projection of the stack, (2) automatically threshold *GBE-Su(H)-lacZ* reporter
177 expression in 3D to determine its expression status (positive or negative) in
178 every esg$^+$ cell, (3) manually identify the nests of esg$^+$ cells so that (4) a series
179 of 3D stacks, containing only one pair each, is automatically cropped, and (5)
180 the contact membrane of each esg$^+$ cell pair is semi-automatically determined
181 using FIJI for each optical plane, by binarising the immunofluorescence of
182 Armadillo/*β*-catenin (Arm). Arm labels the membrane throughout the apical-
183 basal axis (see Results), which allows measuring the amount of contacting
184 membrane in each cell pair as the number of Arm$^+$ voxels shared between the
185 two cells (expressed in μm^2).

For measuring Notch and Arm distribution at the membrane, the membrane contours (3 pixels wide) of cells in pairs were manually determined in each plane. Intensity data from those positions were used as follows:

Intensity normalisation. For each cell pair, two nearby 50x50 pixel squares spanning the full z-stack were manually selected, the signal therein averaged for all the planes where membrane was detectable, and this average value taken as background. Notch and Arm intensity values for that stack were normalised by dividing by the background value.

Distribution along cell perimeter. Each membrane pixel position was assigned an angular value respect to the centroid by calculating its tangent arc (±π depending on the quadrant). Thirty overlapping sliding windows (of 2π/15 rad with half window overlap) were delimited in each plane, and their pixel intensities were normalised and averaged.

Distribution along the apical-basal axis. Each cell was sliced in 10 overlapping angular windows (2π/5 rad with half overlap). For each window, a normalised, average intensity measurement was taken per confocal plane (i.e. along the apical-basal axis). Apical-basal positions were normalised from 0 to 1. Intensity data points along the apical-basal axis were obtained by interpolation from average normalized intensity values.

Results

Lateral inhibition can result in stable, opposing symmetric signalling states

We study the steady-state behaviour of a standard model of lateral inhibition for the case of two cells (see Methods). The steady states of this system depend on two parameters, a and b (the dimensionless activation and inhibition thresholds, respectively; see Methods), which we allow to vary across the population of cell pairs. We then calculate the equilibrium state of the system in this two-dimensional parameter space, according to the resulting signalling profile: asymmetric (one cell positive for Notch activation and the other one negative, see Methods), symmetric positive, or symmetric negative for Notch activation (Fig. 1E). Thus, for a population of cell pairs with

216 variable activation or inhibition thresholds (*a* and *b*), the three possible
217 signalling state profiles occur (Fig. 2A, see Fig. 2B-E for a comparison of the
218 dynamic evolution of examples of the three profiles, with Fig. 2B
219 corresponding to the parameter values from Collier et al., 1996). The three
220 signalling state profiles can be found within a relatively short range of
221 parameter values (Fig. 2A), and this scenario does not change qualitatively
222 when considering a wide range of threshold values for Notch activity
223 classification, as defined in the Methods section ($0.001 \leq N_{thr} \leq 0.7$) (Fig. S1).

224 In a biological system, the existence of three possible signalling state profiles
225 would be equivalent to having three different cell fate combinations across a
226 population of initially uncommitted cell pairs interacting through Notch/Delta,
227 with the specific fate combination of a given cell pair depending on the
228 sensitivity to Delta activation and Notch inhibition of the pair. To investigate
229 the potential of this lateral inhibition model, incorporating variable activation
230 and inhibition thresholds, to describe a real biological system, we turned to the
231 *Drosophila* midgut.

232 *Cell contact area as indicator of activation threshold*

233 In the *Drosophila* midgut, Notch negative cells correspond to ISCs, and Notch
234 positive to EBs. The Notch activity reporter *GBE-Su(H)* is hardly expressed
235 above background levels in ISCs (Ohlstein and Spradling, 2007), and our own
236 observations), and hence our choice of a low threshold value, $N_{thr} = 0.1$.
237 Symmetric positive pairs will equate to an event of symmetric differentiation
238 (EB/EB), symmetric negative pairs to symmetric self-renewal (ISC/ISC) and
239 asymmetric pairs to asymmetric ISC fate (ISC/EB) (Fig. 2A).

240 To relate the model to real tissue, we need first to consider how the
241 dimensionless parameters a and b are related to biological features displaying
242 variability across undifferentiated (esg$^+$) cell pairs. We assume that
243 biochemical processes intrinsic to the cell, such as protein degradation rates
244 (δ_D and δ_N), the maximal biosynthesis rates (α and β), and the threshold of
245 Delta inhibition by Notch in the same cell (K_D), will not be highly variable

among cells with a common developmental identity. On the other hand, the threshold of Notch activation by neighbouring Delta (K_N) depends directly on the interaction between the two cells, which could be variable for different pairs of cells. For instance, due to the spatial constraints of cell packing, the contact area between cell pairs could be substantially different from pair to pair. Indeed, tissue images reveal that undifferentiated cells in nests show irregular shapes and variable contact area (Fig. 3A). In the Notch/Delta system the amounts of Notch and Delta are usually limiting, and this seems to hold true for the adult *Drosophila* gut, where haploinsufficiency has been described (Biteau et al., 2008; de Navascués et al., 2012). Therefore, it is expected that variations of ~2-fold or more in contact area would lead to significant changes in the levels of Notch activation. This is captured in the model by the dimensionless activation threshold a, which can be assumed in a first approximation, following Eqn 7 above, to be inversely related with the contact area (the larger the contact area, the easier it is for Delta to activate Notch, and thus the smaller the activation threshold). As shown in Fig. 2A (see also Fig. S2), variation in a best allows for heterogeneity in stable steady state levels of Notch activity and therefore in fate choice. From this we hypothesize that variation of contact area (or any other biological feature correlating with the threshold of Notch activation) is likely to allow the diversity in fate outcome that we observe in the model.

For this relationship to hold, Notch distribution at the cell membrane must be such that the amount of receptor correlates with the contact area. To evaluate this, we examined the localisation of both Notch and Armadillo/*β*-catenin (Arm) in both single and paired undifferentiated cells (recognised by *Notch* expression; Bardin et al., 2010) of the adult posterior midgut epithelium with confocal microscopy (Fig. 3A). In *Drosophila* epithelia, Arm/*β*-cat participates in the formation of adherens junctions, which localise mostly in an apical domain, with lower levels at the lateral membrane (Tepass and Hartenstein, 1994). Therefore, we used Arm staining to define membrane boundaries in 3D, and measured the intensity of Notch and Arm signals at the cell membrane.

278 We could not find any strong pattern in the variations of Notch
279 immunodetection intensity within confocal planes, and it would only seem that
280 Notch is slightly enriched at the boundary between two esg$^+$ cells (Fig. 3B).
281 This indicates that Notch concentration is largely independent of the position
282 at the membrane along the cell perimeter, and in particular along the contact
283 between esg$^+$ cells. Moreover, the localisation of Notch along the apical-basal
284 axis of the cells is also largely homogeneous. This is manifest in the small
285 variation in the average amounts of Notch between different optical planes
286 (Fig. 3D), and in the narrow distribution of mean values per plane, with low
287 values of coefficients of variation per plane, of Notch intensity values (Fig.
288 S3B,D). Therefore, the contact area between cells is a good approximation to
289 the total amount of Notch receptor available for signalling.

290 We note that Arm largely parallels Notch localisation at the membrane (Figs.
291 3C,E and S3A,C) but shows a stronger enrichment at the boundary (Fig. 3C),
292 in agreement with previous reports (Maeda et al., 2008). Incidentally, these
293 results also reveal that neither Arm nor Notch are restricted to the apical
294 domain in the midgut epithelium**,** and instead can be found in similar amounts
295 along the apical-basal axis of the membrane in ISCs and EBs (Fig. 3D-F).
296 This situation contrasts with Arm and Notch distribution in other *Drosophila*
297 epithelia (Tepass and Hartenstein, 1994; Tepass et al., 2001).

298 Taken together, our results suggest that Notch receptor is randomly
299 distributed in the cell membrane, which suggests that measurements of
300 membrane contact area may be relevant to the dynamics of Delta-Notch
301 signalling as a proxy for the activation threshold a in our model.

302 *Correlation of contact area values and cell fate profiles*

303 We have shown that contact area can be used as a measure of the amount of
304 Notch available for interaction with Delta. We thus measured contact area in
305 508 pairs of esg$^+$ cells with both symmetric (ISC-ISC and EB-EB) and
306 asymmetric (ISC-EB) fates (Fig. 1D-E); these pair classes have been
307 described in (de Navascués et al., 2012; Goulas et al., 2012). We found the
308 contact area in these pairs to be highly variable, ranging from just around

309 1μm^2 to over 60μm^2 (Fig. 4A) and with a high coefficient of variation (0.52).
310 This degree of variability indicates that contact area has the potential to be a
311 regulatory mechanism of the system (through its influence on the
312 dimensionless activation threshold a).

313 Our model predicts that a biological feature influencing Notch/Delta signalling
314 thresholds in cell pairs should correlate with the patterns of symmetric and
315 asymmetric fates. Therefore, we classified measurements of contact area
316 according to the fate profile of their corresponding cell pair and compared their
317 values (Fig. 4B). We found that on average, the contact area between ISC-
318 ISC (11.59 ± 0.73 μm^2; mean ± standard error of the mean) is clearly smaller
319 than those of ISC-EB (17.68 ± 0.42 μm^2) and EB-EB pairs (21.6 ± 2.76 μm^2).
320 This is also clear when considering the distribution of sizes for each pair type
321 and confirmed by the Kolmogorov-Smirnov test (Fig. 4C). From these results
322 we take that ISC-ISC pairs have a significantly smaller contact area than the
323 other two fate profiles.

324 *Updating the model with area variation reproduces fate profile distributions*

325 This finding gives us biological justification to consider the activation threshold
326 a to be variable in the model (inversely proportional to the contact area), and
327 test the capacity of the model to produce the observed proportions of fate
328 pairs. To do this, we first generated a large sample of contact area values *A*,
329 from a Smooth Kernel Distribution based on the experimental data (Fig. 4A).
330 To input values from *A* into the model, we considered the area values *A*
331 inversely related to the activation threshold a by a constant *c* ($a = c/A$),
332 treated as a parameter of the model. We then analysed the stable steady
333 states of the model, obtaining the proportions of the three possible fate pairs
334 resulting from *A*, for different values of *b* and *c*.

335 In order to compare the fate distribution obtained from the model and the
336 experimental data we use the Kullback-Leibler relative entropy (*H*), which is a
337 dissimilarity measure between two probability distributions (giving the value 0
338 if the distributions are equal; Kullback and Leibler, 1951). We found an

339 excellent agreement between the proportions of EB-EB, EB-ISC and ISC-ISC
340 pairs observed experimentally, and the distributions from the model for an
341 extended range of values of *b* and *c*, as indicated by the low values of *H*
342 between theoretical and experimental distributions (Fig. 4D). The best fit
343 (Table 1) is obtained with b=0.19 and c=18 (H=0.3×10^{-3}, black dot in Fig. 4D).
344 By mapping *A* input values (Fig. 4A) for b=0.19 and c=18 to the model phase
345 diagram (horizontal line in Fig. 2A), one finds that ISC-ISC pairs occur at the
346 lowest values of contact area, in good agreement with our experimental
347 observations (Fig. 4B-C). In this region of the parameter space, EB-EB and
348 ISC-EB pairs are found at intermediate or high values of contact area (lower
349 a), respectively. While the model favours EB-EB pairs resulting from smaller
350 contact areas than ISC-EB pairs, we cannot distinguish statistically between
351 the two experimental distributions of contact area (see Fig. 4C). Hence, we
352 propose that the contact area between pairs of cells can influence the fate
353 outcome of Notch/Delta signalling in the *Drosophila* midgut (Fig. 4E), with
354 small contact area clearly favouring symmetric self-renewal.

355 **Discussion**

356 We have considered a standard model of Notch/Delta-mediated lateral
357 inhibition (Collier et al., 1996) and investigated the effect of the trans-
358 activation of Notch by Delta and the inhibition threshold of Delta by Notch
359 signalling (here considered phenomenologically as the dimensionless
360 thresholds a and b, respectively) on the dynamics of lateral inhibition for a
361 system of two cells. We find that, provided there is a degree of variability in
362 signalling thresholds between cell pairs, three different signalling states (and
363 therefore fate combinations) can occur under the same conditions. This is a
364 considerable expansion of the model, whose use has so far been mostly
365 centred on solutions that provide fine-grained (checkerboard) patterns. This
366 population-level variability of signalling thresholds can be associated to
367 diversity in the contact areas between pairs of cells. The model reproduces
368 the signalling outcomes observed in the *Drosophila* intestine, which translate
369 into differentiation vs. self-renewal fates. This in turn provides a mechanism

370 whereby ISCs may undergo neutral competition, which is a widespread
371 pattern of adult tissue maintenance in metazoans from *Drosophila* to humans.
372 These results thus provide a potential biological justification for the neutral
373 competition of *Drosophila* adult ISCs.

374 The seminal work by Collier et al. (1996) established a minimal model which
375 crystallised the biological intuition of lateral inhibition developed from the
376 observation of neurogenesis and akin processes of precursor selection
377 (Sprinzak et al., 2011; Formosa-Jordan et al., 2012; Petrovic et al., 2014):
378 amplification of small differences in signal, leading to checkerboard patterns of
379 stable, all-or-none signalling states. This formalisation, with their parameter
380 choice for a, b, has justly become a reference in the field. In the last few years
381 there have been expansions of this model to accommodate additional
382 features, such as the specific activity of Jagged, another Notch ligand
383 (Boareto et al., 2015), or departures from fine-grained patterns based on
384 different ratios of positive and negative Notch cells (de Back et al., 2013).
385 These models introduce additional genetic components or noise terms that
386 allow the new phenomenology. By contrast, we have left intact the general
387 dynamics of the minimal model of Collier et al. (1996) and introduced only a
388 degree of variability in the sensitivity of each cell pair to signal transduction.

389 Another important contribution of Collier et al. (1996) was to identify the
390 mathematical condition for symmetry breaking. We explore this condition
391 further and determine systematically the contribution of the signalling
392 thresholds a and b to the condition of stability (Fig. 2A). It would also be
393 interesting to explore how variation in the cooperativity of the Notch trans-
394 activation or Delta inhibition (parameters r, h) affect the capability of the
395 system to arrive to symmetric or asymmetric steady states, as seen recently in
396 Turing patterns (Diambra et al., 2015).

397 Our work considers the contact area between cells engaged in signalling as
398 the source of variation in signalling threshold. Contact area can be an
399 effective tuning parameter of a biological system (Khait et al., 2015), since it
400 can integrate mechanical constraints into signalling, as it has been shown for

401 cell density and proliferative control by the Hippo pathway (Schlegelmilch et
402 al., 2011; Kim et al., 2011; Silvis et al., 2011). In a system such as the
403 posterior midgut, where some differentiated cells are much larger than their
404 progenitors (see Fig. 1A), differentiated and mature cell loss certainly would
405 have a local impact in the packing geometry of cells interacting via
406 Notch/Delta, and connect naturally with the fate outcome of stem cell
407 divisions. This could be particularly useful in conditions of regeneration.
408 Importantly, our theoretical framework could in principle accommodate any
409 source of variation; for instance, variation arising from the unequal (either
410 random or regulated) inheritance of signalling components could result in
411 variation in the capability of signal transduction in the population. It is
412 interesting to consider that while shortly after division most of the ISC
413 daughter cells display similar levels of Notch and Delta proteins (Ohlstein and
414 Spradling, 2007), endosomes bearing the signalling molecule Sara display an
415 inhomogeneous inheritance pattern (Montagne and González-Gaitán, 2014). It
416 has recently been found that ISC divisions producing enteroendocrine cell
417 precursors do segregate Delta asymmetrically towards the precursor cell (Guo
418 and Ohlstein, 2015), which suggests that ISCs switch between different types
419 of cell division.

420 Understanding how Notch/Delta signalling results in stochastic cell fate
421 patterns is of particular relevance in adult homeostatic tissues, as Notch
422 signalling controls fate in many types of tissue stem cells (Koch et al., 2013).
423 Moreover, many adult stem cells balance their fate via neutral competition
424 (Krieger and Simons, 2015). Our model proposes a mechanism whereby
425 Notch/Delta signalling could result in neutral competition of stem cells by
426 lateral inhibition between sibling cells. This provides an alternative explanation
427 to the neutral competition of Drosophila adult ISCs, which has been proposed
428 to arise from Notch/Delta-mediated lateral inhibition involving the offspring of
429 non-related ISCs, coinciding in space (de Navascués et al., 2012) and
430 resolving 20% of the time in symmetric fate. However, that proposal faces the
431 difficulty that ISC/EB nests rarely contain more than two cells (de Navascués
432 et al., 2012). Moreover, we and others have found isolated pairs of ISCs or

EBs frequently in the tissue (de Navascués et al., 2012; Goulas et al., 2012). Our model provides a potential explanation of how the offspring of a single ISC (pairs of Notch/Delta signalling cells) may reach a symmetric steady state, leading to symmetric self-renewal o differentiation.

It would be interesting to see how our model (based on signalling threshold variability) translates to a larger group of interacting cells, in particular in light of recent findings in the esophageal epithelium. There, tissue is maintained by the neutral competition of basal progenitor cells (Doupé et al., 2012), and this competition is heavily influenced by Notch signalling, to the point that alterations in the pathway can lead to the fixation of mutant clones and poise the tissue for tumour initiation (Alcolea et al., 2014).

Acknowledgements

We wish to acknowledge support from CONICET to NG and from Cardiff University to JdN. JGO and RMC are supported by the Spanish Ministerio de Economía y Competitividad and FEDER, through project FIS2012-13360-C02-01, and the ICREA Academia Programme. RMC also acknowledges financial support from La Caixa Foundation. We would like to thank Alfonso Martínez Arias for his encouragement and support and Nicole Gorfinkiel and David Sprinzak for critical comments on the manuscript.

Competing Interests

No competing interests declared.

454 **Figure Legends**

455 **Figure 1**. Tissue maintenance in the Drosophila adult midgut. Scale bars:
456 20μm. A. Confocal micrograph showing the cell types present in the midgut
457 epithelium. ISCs are esg-GFP+ (blue) and EBs are esg-GFP+ and
458 GBE-Su(H)-lacZ+ (green). The two differentiated cells, enteroendocrine cells
459 and enterocytes, are recognisable by Prospero (pros) expression and having
460 large, polyploid nuclei (Hoechst, grey), respectively. B-C. ISCs self renew and
461 produce EBs (which will terminally differentiate without further division) (B), by
462 dividing either asymmetrically (one ISC and an EB), or symmetrically into two
463 ISCs or two EBs (C). D. Distribution of cell fates for nests containing two
464 undifferentiated cells (N=508). ISC-ISC pairs (blue, N=74), EB-EB pairs
465 (green, N=28) and ISC-EB pairs (orange, N=406). E. Confocal micrographs
466 showing examples of cell pair fate profiles: asymmetric (i), symmetric Notch
467 negative (two ISCs, ii) and symmetric Notch positive (two EBs, iii).

468 **Figure 2**. Parameter space and dynamic behaviour of the model. A. Stable
469 solutions of the system classified according to their resulting signalling state.
470 Green stands for symmetric positive fates (EB-EB pairs), blue represents
471 symmetric negative fates (ISC-ISC pairs), and orange denotes asymmetric
472 fates (ISC-EB pairs). The threshold in Notch level for EB identification is taken
473 to be equal to 0.1 (see the text for more details). The short, horizontal line
474 indicates 95% of “a” values used to generate a theoretical distribution of cell
475 fates for b=0.19 (see main text). Dotted line, boundary of stability for steady
476 states with identical cells; these ‘homogeneous’ solutions are stable above the
477 line. B-E. Time evolution (in arbitrary units) of Notch and Delta activity in pairs
478 of cells interacting with parameters from the points indicated as 1 to 4 in (A).
479 Parameter values in point 1 correspond to those used in Collier et al. (1996)
480 (B), while parameter values in points 2-4 (C-E) correspond to examples of
481 other asymmetric pairs, and symmetric positive and symmetric negative pairs.

482 **Figure 3**. Variability in contact area and distribution of Notch at the
483 membrane. A. Confocal stacks projected in Z, showing variability in contact
484 length (as proxy for area). Scale bar: 20μm. B-C. Notch (B) and Arm (C) levels

485 along the perimeter of the cell planes (colour lines) and mean (white). For
486 each cell plane, position 0 corresponds to the centre of the contacting
487 membranes (defined as the position that intersects the line connecting the cell
488 centroids in that plane). D-E. Notch (D) and Arm (E) levels along the apical-
489 basal cell axis (with height of the cell normalised to 1). Each cell contributes
490 ten lines to the plot, corresponding to the intensity values along the vertical
491 axis of non-overlapping, angular windows of 2π/10. Data displayed in B-E are
492 from 20 paired esg+ cells. Data in B-E are from 20 paired cells. F. (i, ii) Side
493 views of the intestinal epithelium, showing the apical-basal distribution of
494 Notch and Arm. Lumen is at the top and basal at the bottom. (iii-v) Top view of
495 the intestinal epithelium (iii) with ZY and XZ side views (iv, v) corresponding to
496 the marked lines in (iii). Scale bar in (ii): 10μm.

497 **Figure 4**. The model can reproduce the observed cell fate profiles. Data set
498 from N=508 nests (Fig. 1D). A. Frequency of contact area values for nests of
499 two undifferentiated cells. Line marks the Smooth Kernel Distribution (SKD)
500 used to generate areas for the simulation. B. Contact area values segregated
501 by fate profiles. Black lines indicate mean values. Grey lines mark the position
502 of one standard deviation below or above the mean. C. Cumulative frequency
503 of the contact area data displayed in (B). Note that ISC-EB and EB-EB
504 distributions cannot be distinguished statistically. D. Kullback-Leibler relative
505 entropy (H) between experimental and model distributions as a function of b
506 and c. Values of area in the model are generated by the SKD depicted in (A).
507 Best value corresponds to b=0.19 and c=18 (black dot) and leads to fate
508 profile proportions as in Table 1. E. Fate outputs for the lateral inhibition
509 model for three different values of the contact area.

References

Alcolea, M. P., Greulich, P., Wabik, A., Frede, J., Simons, B. D. and Jones, P. H. (2014). Differentiation imbalance in single oesophageal progenitor cells causes clonal immortalization and field change. *Nature Cell Biology* **16**, 615–622.

Arias, A. M. and Stewart, A. (2002). *Molecular Principles of Animal Development*. Oxford University Press, USA.

Artavanis-Tsakonas, S., Rand, M. D. and Lake, R. J. (1999). Notch signaling: cell fate control and signal integration in development. *science (New York, NY)* **284**, 770–776.

Baker, A.-M., Cereser, B., Melton, S., Fletcher, A. G., Rodriguez-Justo, M., Tadrous, P. J., Humphries, A., Elia, G., McDonald, S. A. C., Wright, N. A., et al. (2014). Quantification of crypt and stem cell evolution in the normal and neoplastic human colon. *CellReports* **8**, 940–947.

Bardin, A. J., Perdigoto, C. N., Southall, T. D., Brand, A. H. and Schweisguth, F. (2010). Transcriptional control of stem cell maintenance in the Drosophila intestine. *Development* **137**, 705–714.

Biteau, B., Hochmuth, C. E. and Jasper, H. (2008). JNK activity in somatic stem cells causes loss of tissue homeostasis in the aging Drosophila gut. *Cell Stem Cell* **3**, 442–455.

Boareto, M., Jolly, M. K., Lu, M., Onuchic, J. N., Clementi, C. and Ben-Jacob, E. (2015). Jagged–Delta asymmetry in Notch signaling can give rise to a Sender/Receiver hybrid phenotype. *Proceedings of the National Academy of Sciences* **112**, E402–E409.

Bray, S. and Furriols, M. (2001). Notch pathway: making sense of suppressor of hairless. *Curr Biol* **11**, R217–21.

Collier, J. R., Monk, N. A., Maini, P. K. and Lewis, J. H. (1996). Pattern formation by lateral inhibition with feedback: a mathematical model of delta-notch intercellular signalling. *J Theor Biol* **183**, 429–446.

de Back, W., Zhou, J. X. and Brusch, L. (2013). On the role of lateral stabilization

during early patterning in the pancreas. *Journal of The Royal Society Interface* **10**, 20120766.

de Navascués, J., Perdigoto, C. N., Bian, Y., Schneider, M. H., Bardin, A. J., Martinez-Arias, A. and Simons, B. D. (2012). Drosophila midgut homeostasis involves neutral competition between symmetrically dividing intestinal stem cells. *EMBO J* **31**, 2473–2485.

Diambra, L., Senthivel, V. R., Menendez, D. B. and Isalan, M. (2015). Cooperativity to increase Turing pattern space for synthetic biology. *ACS Synth Biol* **4**, 177–186.

Doupé, D. P., Alcolea, M. P., Roshan, A., Zhang, G., Klein, A. M., Simons, B. D. and Jones, P. H. (2012). A Single Progenitor Population Switches Behavior to Maintain and Repair Esophageal Epithelium. *science (New York, NY)* **337**, 1091–1093.

Ehebauer, M., Hayward, P. and Arias, A. M. (2006). Notch, a universal arbiter of cell fate decisions. *science (New York, NY)* **314**, 1414–1415.

Formosa-Jordan, P., Ibanes, M., Ares, S. and Frade, J. M. (2012). Regulation of neuronal differentiation at the neurogenic wavefront. *Development* **139**, 2321–2329.

Goulas, S., Conder, R. and Knoblich, J. A. (2012). The Par Complex and Integrins Direct Asymmetric Cell Division in Adult Intestinal Stem Cells. *Cell Stem Cell* **11**, 529–540.

Greenwald, I. (1998). LIN-12/Notch signaling: lessons from worms and flies. *Genes & Development* **12**, 1751–1762.

Guo, Z. and Ohlstein, B. (2015). Bidirectional Notch signaling regulates Drosophila intestinal stem cell multipotency. *science (New York, NY)* **350**, aab0988–aab0988.

Khait, I., Orsher, Y., Golan, O., Binshtok, U., Gordon-Bar, N., Amir- Zilberstein, L. and Sprinzak, D. (2015). Quantitative analysis of Delta-like-1 membrane dynamics elucidates the role of contact geometry on Notch signaling. *cell reports* **In Press**, 1–27.

Kim, N.-G., Koh, E., Chen, X. and Gumbiner, B. M. (2011). E-cadherin mediates contact inhibition of proliferation through Hippo signaling-pathway components. *Proceedings of the National Academy of Sciences* **108**, 11930–11935.

Klein, A. M. and Simons, B. D. (2011). Universal patterns of stem cell fate in cycling adult tissues. *Development* **138**, 3103–3111.

Koch, U., Lehal, R. and Radtke, F. (2013). Stem cells living with a Notch. *Development* **140**, 689–704.

Krieger, T. and Simons, B. D. (2015). Dynamic stem cell heterogeneity. *Development* **142**, 1396–1406.

Kullback, S. and Leibler, R. A. (1951). On Information and Sufficiency. *Ann. Math. Statist.* 79–86.

Maeda, K., Takemura, M., Umemori, M. and Adachi-Yamada, T. (2008). E-cadherin prolongs the moment for interaction between intestinal stem cell and its progenitor cell to ensure Notch signaling in adult Drosophila midgut. *Genes Cells* **13**, 1219–1227.

Micchelli, C. A. and Perrimon, N. (2006). Evidence that stem cells reside in the adult Drosophila midgut epithelium. *Nature* **439**, 475–479.

Miller, K. G., Field, C. M. and Alberts, B. M. (1989). Actin-binding proteins from Drosophila embryos: a complex network of interacting proteins detected by F-actin affinity chromatography. *The Journal of Cell Biology* **109**, 2963–2975.

Montagne, C. and González-Gaitán, M. (2014). Sara endosomes and the asymmetric division of intestinal stem cells. *Development* **141**, 2014–2023.

Muñoz-Descalzo, S., Tkocz, K., Balayo, T. and Arias, A. M. (2011). Modulation of the ligand-independent traffic of Notch by Axin and Apc contributes to the activation of Armadillo in Drosophila. *Development* **138**, 1501–1506.

Ohlstein, B. and Spradling, A. (2006). The adult Drosophila posterior midgut is maintained by pluripotent stem cells. *Nature* **439**, 470–474.

Ohlstein, B. and Spradling, A. (2007). Multipotent Drosophila intestinal stem cells

specify daughter cell fates by differential notch signaling. *science (New York, NY)* **315**, 988–992.

Othmer, H. G. and Scriven, L. E. (1971). Instability and dynamic pattern in cellular networks. *J Theor Biol* **32**, 507–537.

Petrovic, J., Formosa-Jordan, P., Luna-Escalante, J. C., Abello, G., Ibanes, M., Neves, J. and Giraldez, F. (2014). Ligand-dependent Notch signaling strength orchestrates lateral induction and lateral inhibition in the developing inner ear. *Development* **141**, 2313–2324.

Plahte, E. (2001). Pattern formation in discrete cell lattices. *J Math Biol* **43**, 411–445.

Quiñones-Coello, A. T., Petrella, L. N., Ayers, K., Melillo, A., Mazzalupo, S., Hudson, A. M., Wang, S., Castiblanco, C., Buszczak, M., Hoskins, R. A., et al. (2007). Exploring strategies for protein trapping in Drosophila. *Genetics* **175**, 1089–1104.

Rouault, H. and Hakim, V. (2012). Different Cell Fates from Cell-Cell Interactions: Core Architectures of Two-Cell Bistable Networks. *Biophysj* **102**, 417–426.

Schlegelmilch, K., Mohseni, M., Kirak, O., Pruszak, J., Rodriguez, J. R., Zhou, D., Kreger, B. T., Vasioukhin, V., Avruch, J., Brummelkamp, T. R., et al. (2011). Yap1 acts downstream of α-catenin to control epidermal proliferation. *Cell* **144**, 782–795.

Shaya, O. and Sprinzak, D. (2011). From Notch signaling to fine-grained patterning: Modeling meets experiments. *Curr. Opin. Genet. Dev.* 1–8.

Silvis, M. R., Kreger, B. T., Lien, W.-H., Klezovitch, O., Rudakova, G. M., Camargo, F. D., Lantz, D. M., Seykora, J. T. and Vasioukhin, V. (2011). α-catenin is a tumor suppressor that controls cell accumulation by regulating the localization and activity of the transcriptional coactivator Yap1. *Science Signaling* **4**, ra33–ra33.

Simons, B. D. and Clevers, H. (2011). Strategies for homeostatic stem cell self-renewal in adult tissues. *Cell* **145**, 851–862.

Simpson, P. (2001). Notch signalling in development: on equivalence groups and

asymmetric developmental potential. *Curr. Opin. Genet. Dev.* **7**, 537–542.

Sprinzak, D., Lakhanpal, A., LeBon, L., Garcia-Ojalvo, J. and Elowitz, M. B. (2011). Mutual Inactivation of Notch Receptors and Ligands Facilitates Developmental Patterning. *PLoS Comput Biol* **7**, e1002069.

Sprinzak, D., Lakhanpal, A., LeBon, L., Santat, L. A., Fontes, M. E., Anderson, G. A., Garcia-Ojalvo, J. and Elowitz, M. B. (2010). Cis-interactions between Notch and Delta generate mutually exclusive signalling states. *Nature* **465**, 86–90.

Tepass, U. and Hartenstein, V. (1994). The Development of Cellular Junctions in the Drosophila Embryo. *Developmental Biology* **161**, 563–596.

Tepass, U., Tanentzapf, G., Ward, R. and Fehon, R. (2001). Epithelial cell polarity and cell junctions in Drosophila. *Annu Rev Genet* **35**, 747–784.

Vermeulen, L. and Snippert, H. J. (2014). Stem cell dynamics in homeostasis and cancer of the intestine. *Nat Rev Cancer* 1–13.

Vermeulen, L., Morrissey, E., van der Heijden, M., Nicholson, A. M., Sottoriva, A., Buczacki, S., Kemp, R., Tavaré, S. and Winton, D. J. (2013). Defining stem cell dynamics in models of intestinal tumor initiation. *science (New York, NY)* **342**, 995–998.

Zeng, X. and Hou, S. X. (2015). Enteroendocrine cells are generated from stem cells through a distinct progenitor in the adult Drosophila posterior midgut. *Development* **142**, 644–653.

Figure 1

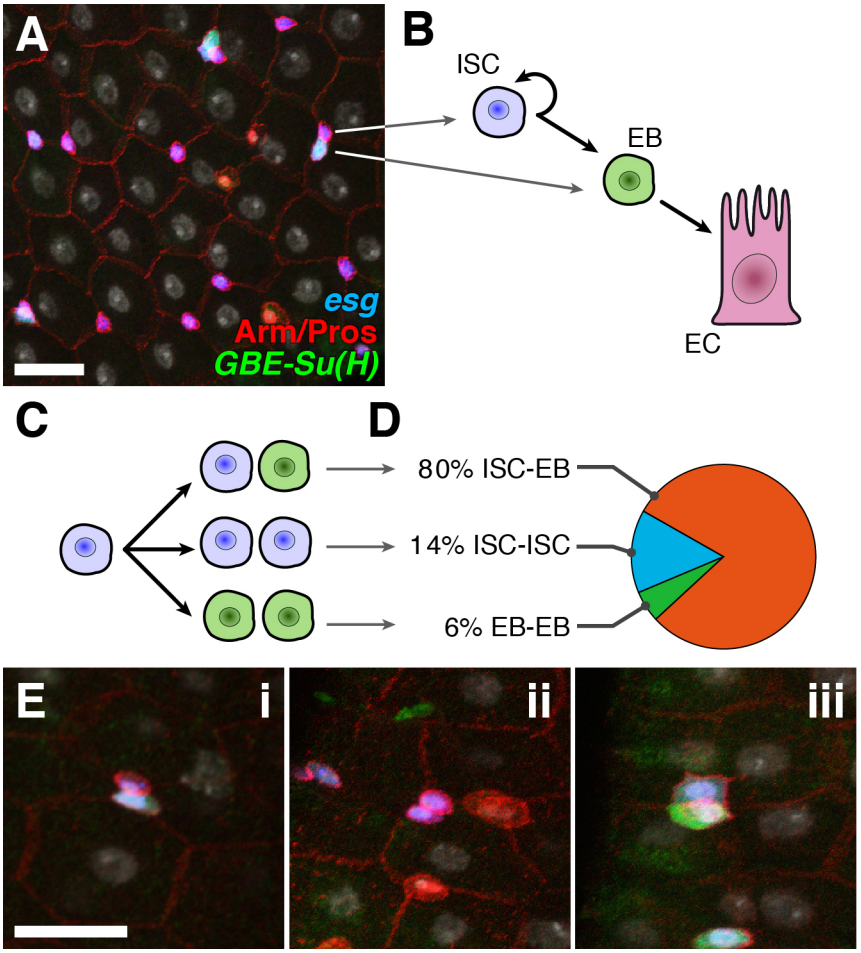
A
esg
Arm/Pros
GBE-Su(H)
B
ISC
EB
EC
C
D
80% ISC-EB
14% ISC-ISC
6% EB-EB
E
i
ii
iii

Figure 2

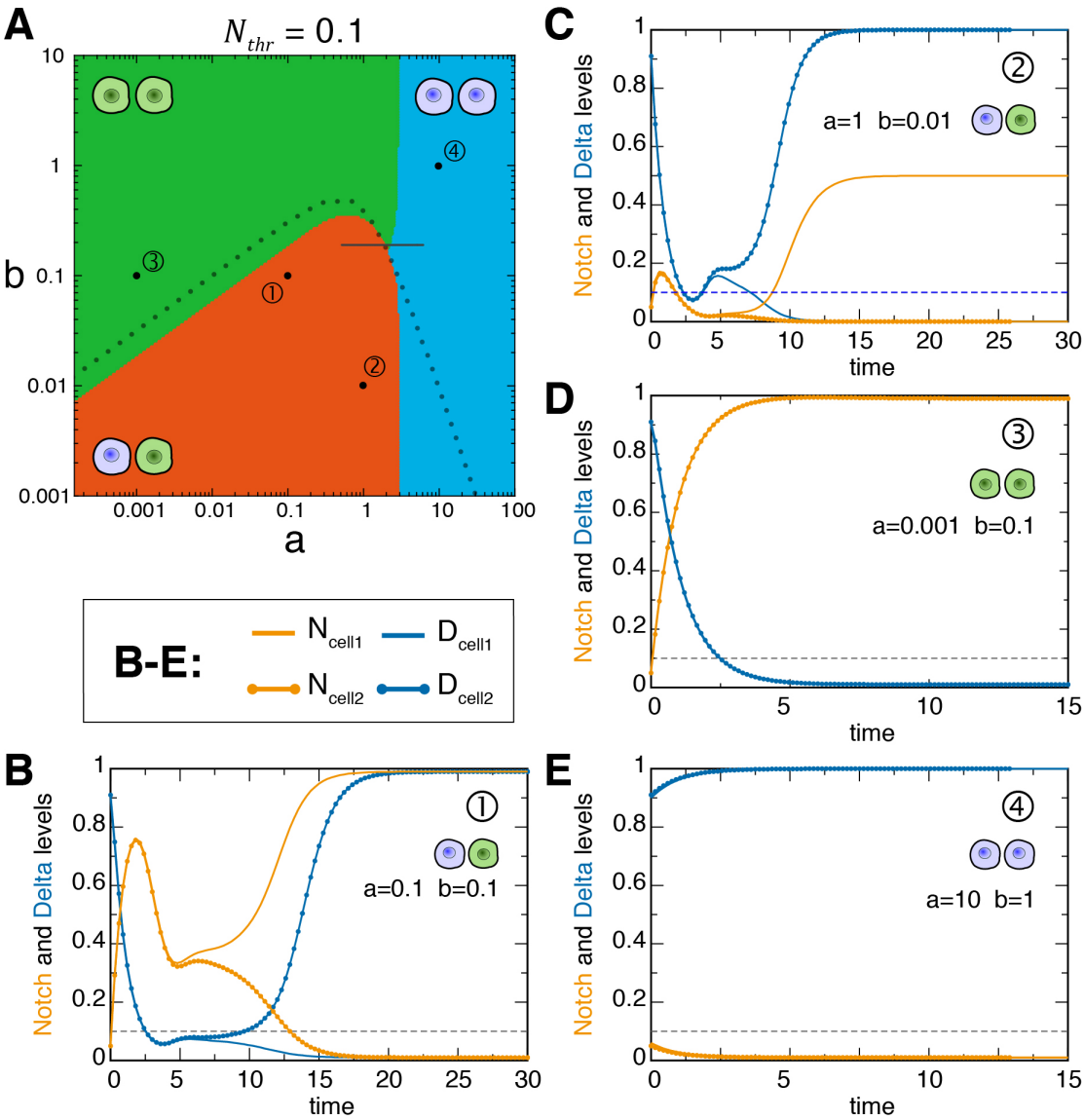
A
N_{thr} = 0.1
b
a
B-E:
N_{cell1}
D_{cell1}
N_{cell2}
D_{cell2}
B
a=0.1 b=0.1
C
a=1 b=0.01
D
a=0.001 b=0.1
E
a=10 b=1
Notch and Delta levels
time

Figure 3

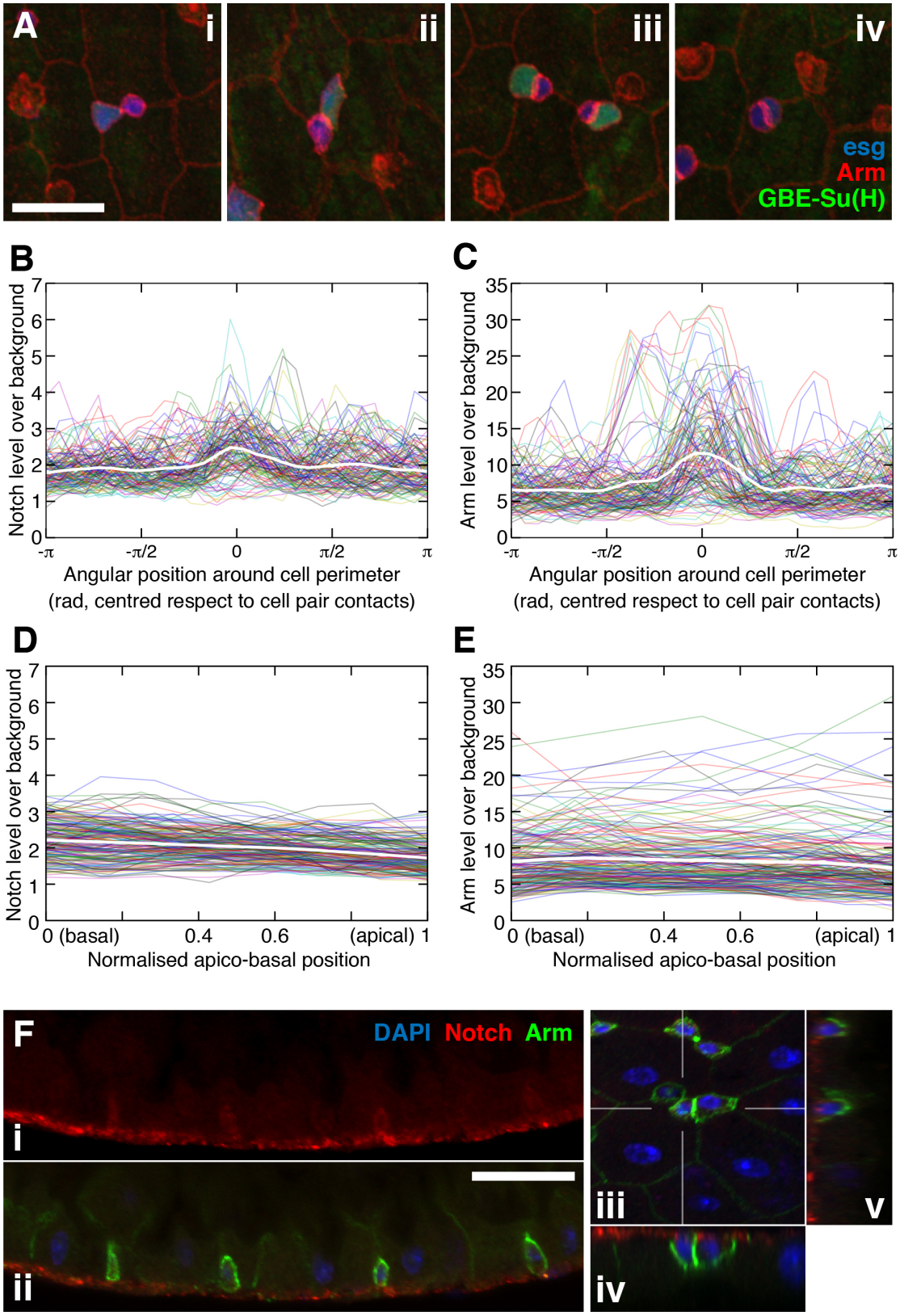
A
i
ii
iii
iv
esg
Arm
GBE-Su(H)
B
Notch level over background
Angular position around cell perimeter
(rad, centred respect to cell pair contacts)
C
Arm level over background
Angular position around cell perimeter
(rad, centred respect to cell pair contacts)
D
Notch level over background
0 (basal)
(apical) 1
Normalised apico-basal position
E
Arm level over background
0 (basal)
(apical) 1
Normalised apico-basal position
F
DAPI Notch Arm
i
ii
iii
iv
v

Figure 4

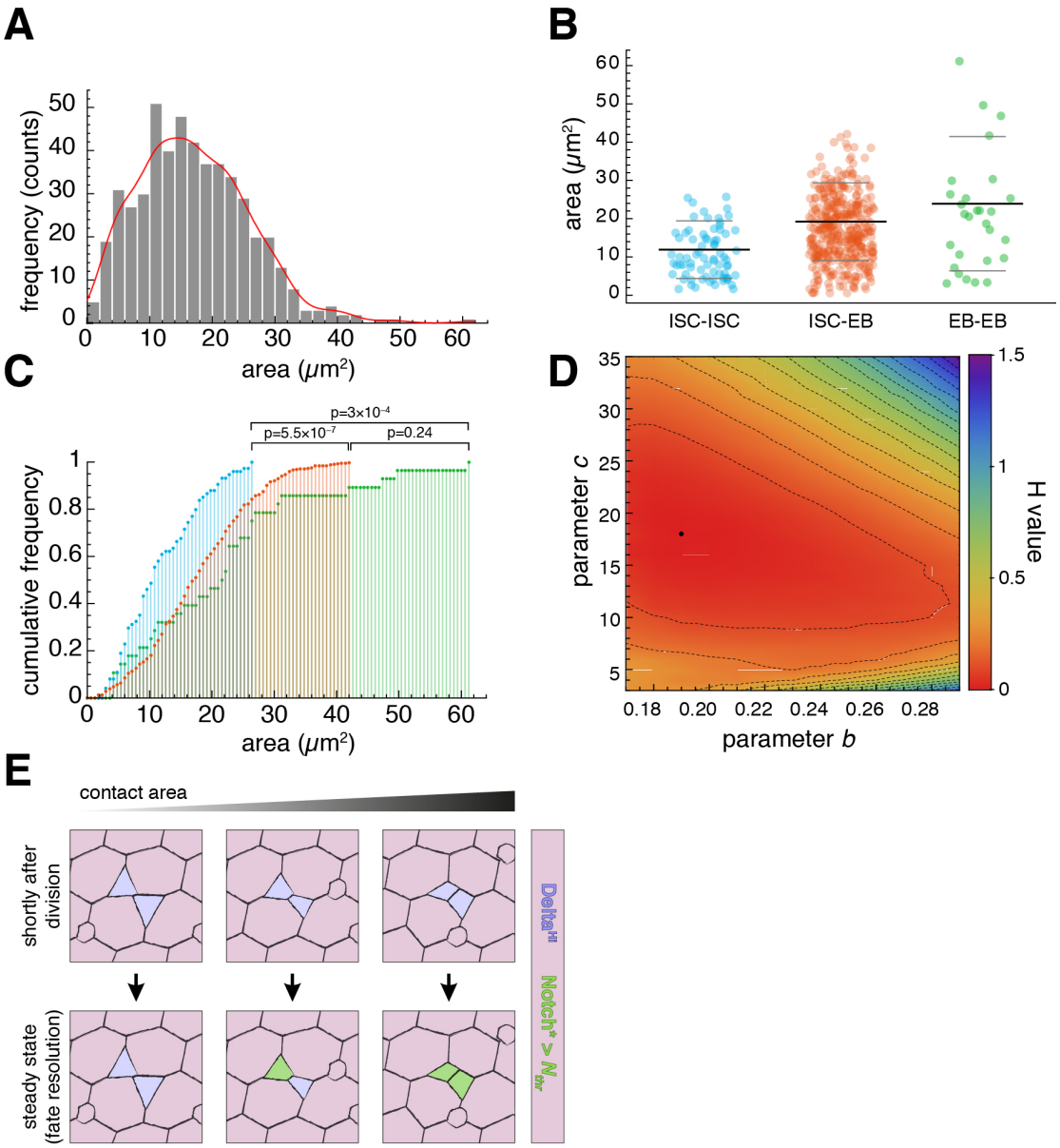
A
frequency (counts)
area (μm²)
B
area (μm²)
ISC-ISC
ISC-EB
EB-EB
C
cumulative frequency
area (μm²)
p=3×10⁻⁴
p=5.5×10⁻⁷
p=0.24
D
parameter c
parameter b
H value
E
contact area
shortly after division
steady state (fate resolution)
Delta
Notch

Table 1. Cell-fate profiles as obtained experimentally and theoretically. The value of Kullback-Leibler relative entropy between the two distributions is 0.3×10^{-3}. Model parameters: b=0.19 and c=18.

pair fate	experimental	model
ISC-ISC	14.6 %	15.1%
EB-EB	5.5 %	5.0 %
ISC-EB	79.9 %	79.9%

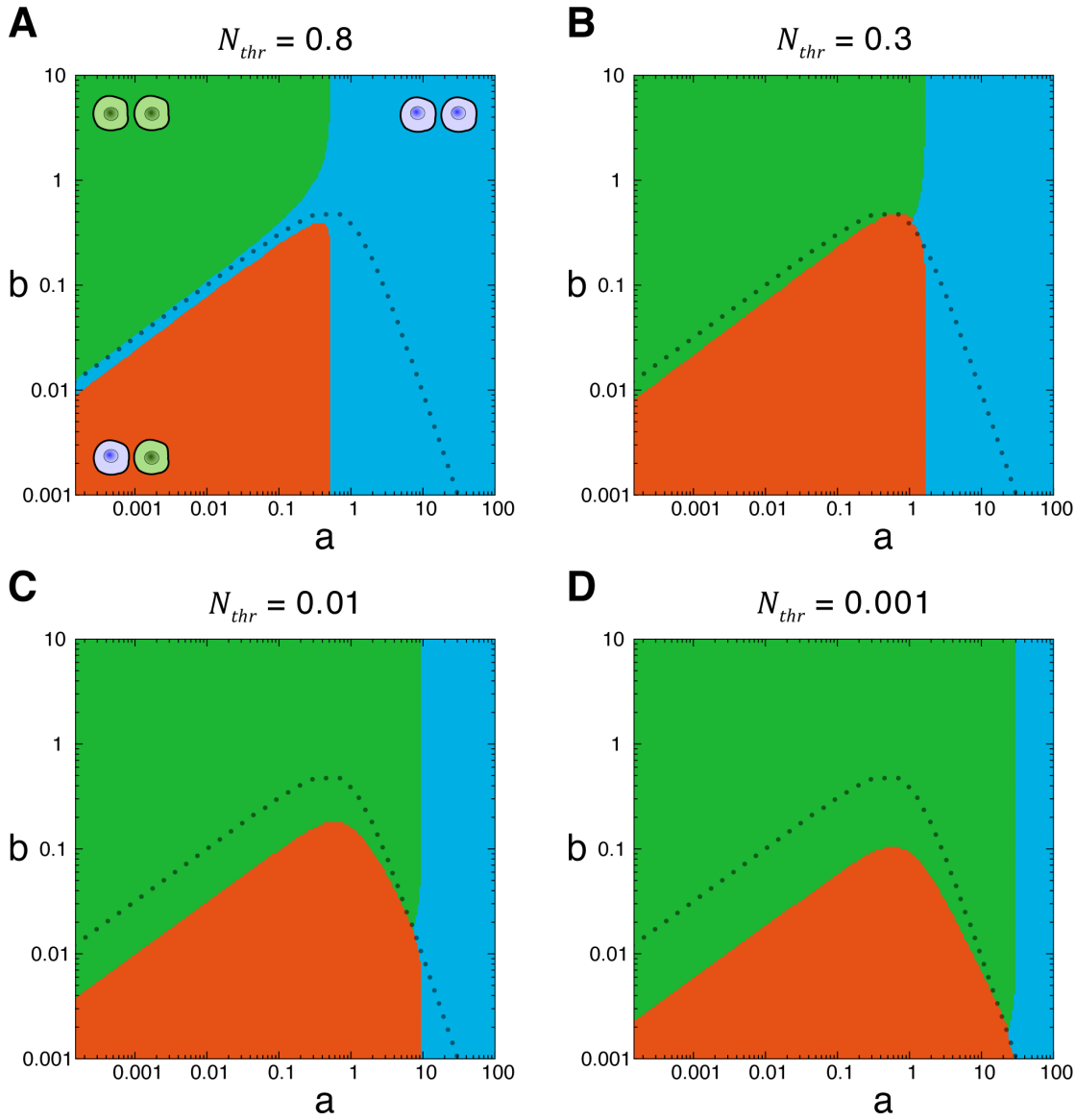

Supplementary Figure 1. Fate profiles in parameter space over a broad range of threshold N_{thr} values. **A-D.** Phase space for N_{thr} equal to 0.8 (A), 0.3 (B), 0.01 (C), and 0.001 (D), respectively. The dotted line marks the stability boundary for the 'homogeneous' solutions (pairs of identical cells), and serves as reference for comparison with Figure 2A. While in A (where $N_{thr} > 0.7$), the area of asymmetric fate is surrounded by symmetric negative resolution, in B-D the organisation of the phase space is very similar, with the transitions shifting along the stability boundary.

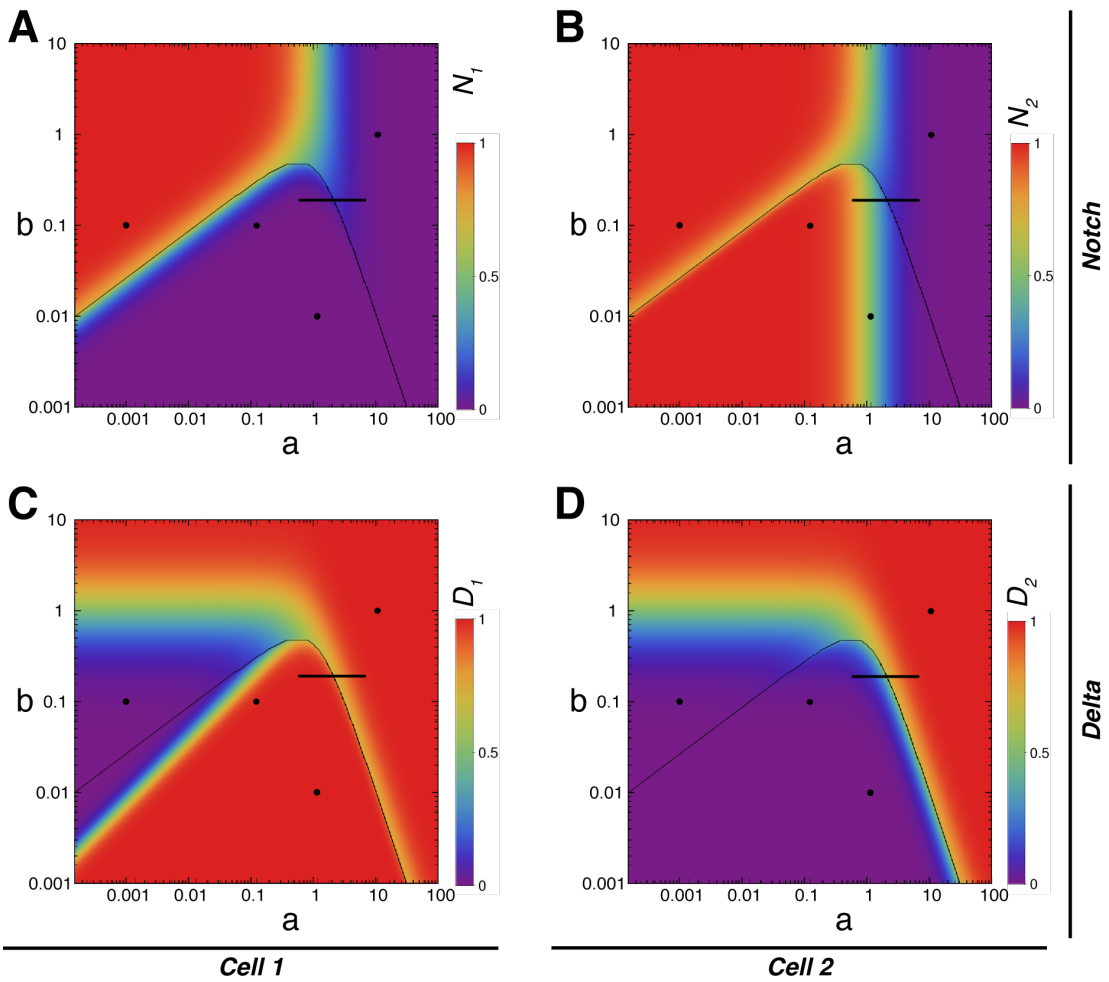

Supplementary Figure 2. Values of Notch and Delta at steady state across parameter space. The short, horizontal line indicates 95% of "a" values used to generate a theoretical distribution of cell fates for b=0.19 (see main text). Dotted line, boundary of stability for steady states with identical cells. The black dots mark the parameter values used in (Collier et al., 1996) (Figure 2B) and the asymmetric, symmetric positive and symmetric negative pairs from Figure 2C-E. **A, B.** Steady-state values of activated Notch the two cells of a pair (one in each panel) respect to a, b. **C-D.** Steady-state values of Delta in the two cells of a pair (one in each panel) respect to a, b. Note that depending on the value of activated Notch, one can find symmetric negative or symmetric positive fate profiles below the boundary (region of heterogeneous solution), showing that the model allows for symmetric steady states where cells in a pair do not have identical amounts of Notch or Delta.

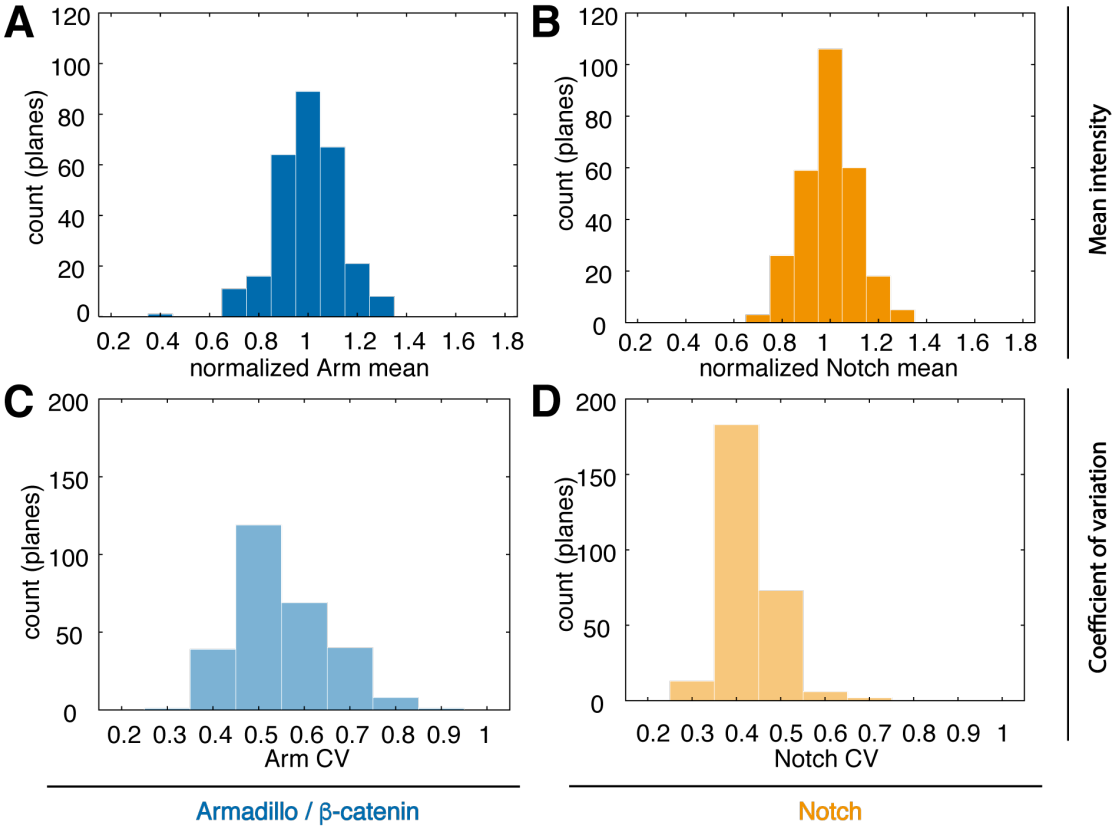

Supplementary Figure 3. Distribution of Notch and Armadillo at the membrane. Data correspond to all 46 analysed cells (single and paired). **A-D.** Histograms of the normalised mean intensity per plane (A, B) and the coefficient of variation (CV) per plane (C, D) for Notch (A, C) and Armadillo (B, D) markers. The normalised mean intensity in plane *i* is defined as the ratio of the average of the plane and the average for the cell.